

## SUPPLEMENTARY INFORMATION

### **Measuring Trapped DNA at the Liquid-Air Interface for Enhanced Single Molecule Sensing**

Nasim Farajpour<sup>1</sup>, Lauren Lastra<sup>1</sup>, Vinay Sharma<sup>1</sup>, Kevin J. Freedman<sup>1\*</sup>

<sup>1</sup>Department of Bioengineering, University of California Riverside, Riverside, CA 92521, USA.

Corresponding author: [\\*kfreedman@engr.ucr.edu](mailto:kfreedman@engr.ucr.edu)

#### Note S1. Mounting Procedure and TEM Imaging

After fabrication of nanopores using the pipette puller device, nanopipette was mounted onto the TEM grid using two-part epoxy glue to make an adhesive surface. Specifically, the TEM grid was held using tweezers and epoxy glue was applied to the grid.

Next, the grid with epoxy was set under an optical microscope and the nanopore was moved near the epoxy using a micrometer. Subsequently, the tip was secured inside the grid under the optical microscope ensuring that the pore opening does not touch the epoxy. The setup was held to dry for 10 minutes and then the nanopore was gently broken away from the grid, leaving just the nanopore inside the TEM grid.

Lastly, gold sputter coating was applied to the nanopores mounted on the grid before the TEM imaging. Thermo Fisher Scientific Tecnai12 Transmission Electron Microscope was utilized for nanopores imaging and characterization. The machine employs Lanthanum Hexaboride as the electron source operated at 120 kV voltage.

## Note S2. Estimating the liquid-air interface during the depth-dependent experiments

A micrometer attached to a pipette holder was used to move the capillaries at different depths inside the solution. In order to estimate the liquid-air interface or the “zero” depth, the nanopore was held outside the solution but within the proximity to the liquid-air interface. Following by applying a constant voltage (between 100 to 200 mV), nanopore was moved toward the surface using the micrometer. We were monitoring the open pore current simultaneously, the point which the current jumped from zero was set on micrometer as the “zero” surface. This adjustment process was repeated during each set of experiments.

Table S1. Pulling Parameters for Fabrication of Borosilicate Nanopores

1) (P-2000, Borosilicate ID 0.5 mm- 22 nm)

Cycle 1: HEAT, 350; FIL,4; VEL, 30; DEL, 200; PUL, 0  
Cycle 2: HEAT, 350; FIL,4; VEL, 30; DEL, 200; PUL, 0  
Cycle 3: HEAT, 350; FIL,4; VEL, 30; DEL, 200; PUL, 0  
Cycle 4: HEAT, 400; FIL,4; VEL, 30; DEL, 126; PUL, 220

2) (P-2000, Borosilicate ID 0.5 mm- 30 nm)

Cycle 1: HEAT, 350; FIL,4; VEL, 30; DEL, 200; PUL, 0  
Cycle 2: HEAT, 350; FIL,4; VEL, 30; DEL, 200; PUL, 0  
Cycle 3: HEAT, 350; FIL,4; VEL, 30; DEL, 200; PUL, 0  
Cycle 4: HEAT, 400; FIL,4; VEL, 30; DEL, 126; PUL, 210

3) (P-2000, Borosilicate ID 0.5 mm- 46 nm)

Cycle 1: HEAT, 350; FIL,4; VEL, 30; DEL, 200; PUL, 0  
Cycle 2: HEAT, 350; FIL,4; VEL, 30; DEL, 200; PUL, 0  
Cycle 3: HEAT, 350; FIL,4; VEL, 30; DEL, 200; PUL, 0  
Cycle 4: HEAT, 400; FIL,4; VEL, 30; DEL, 126; PUL, 200

4) (P-97, Borosilicate ID 0.78 mm - 22 nm)

Cycle 1: HEAT, 584; VEL, 40; TIME, 80; PUL, 65

### Note S3. Finite Element Analysis Modeling

Finite element analysis was performed using COMSOL Multiphysics software. The geometries were created based on a 2D axisymmetric model using a stationary study. The electrostatics physics interface was utilized for electric field modeling. The electrostatics boundary condition for the borosilicate glass was set at a surface charge density of  $-5\text{E-}4 \text{ C/m}^2$ .<sup>1</sup> In order to calculate the FWHM, the electric field norm data at the nanopore was used. The nanopore geometry, salt concentration and applied potential were considered same as experimental parameters.

The  $\alpha$  values were measured to simulate the nanopores with distinct taper lengths. Specifically, the nanopores were first imaged under the optical microscope with the maximum magnification, then the cone half angles were measured using the ImageJ software.

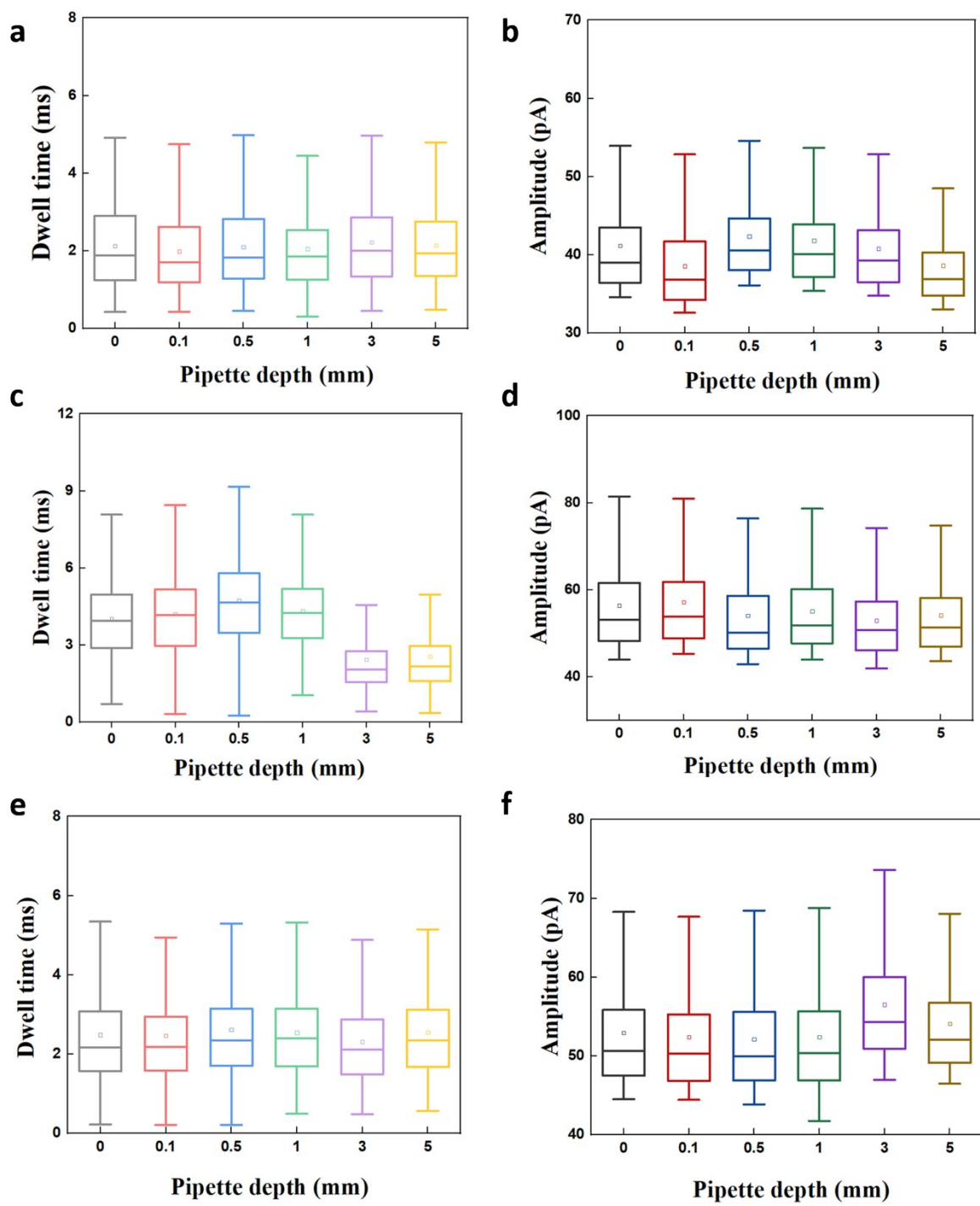


Figure S1. DNA translocation data as a function of depth at 500 mV applied voltage. (a and b) Dwell time and current drop distributions for 22nm size nanopore. (c and d) Dwell time and current drop distributions for 30 nm size nanopore. (e and f) Dwell time and current drop distributions for 46 nm size nanopore.

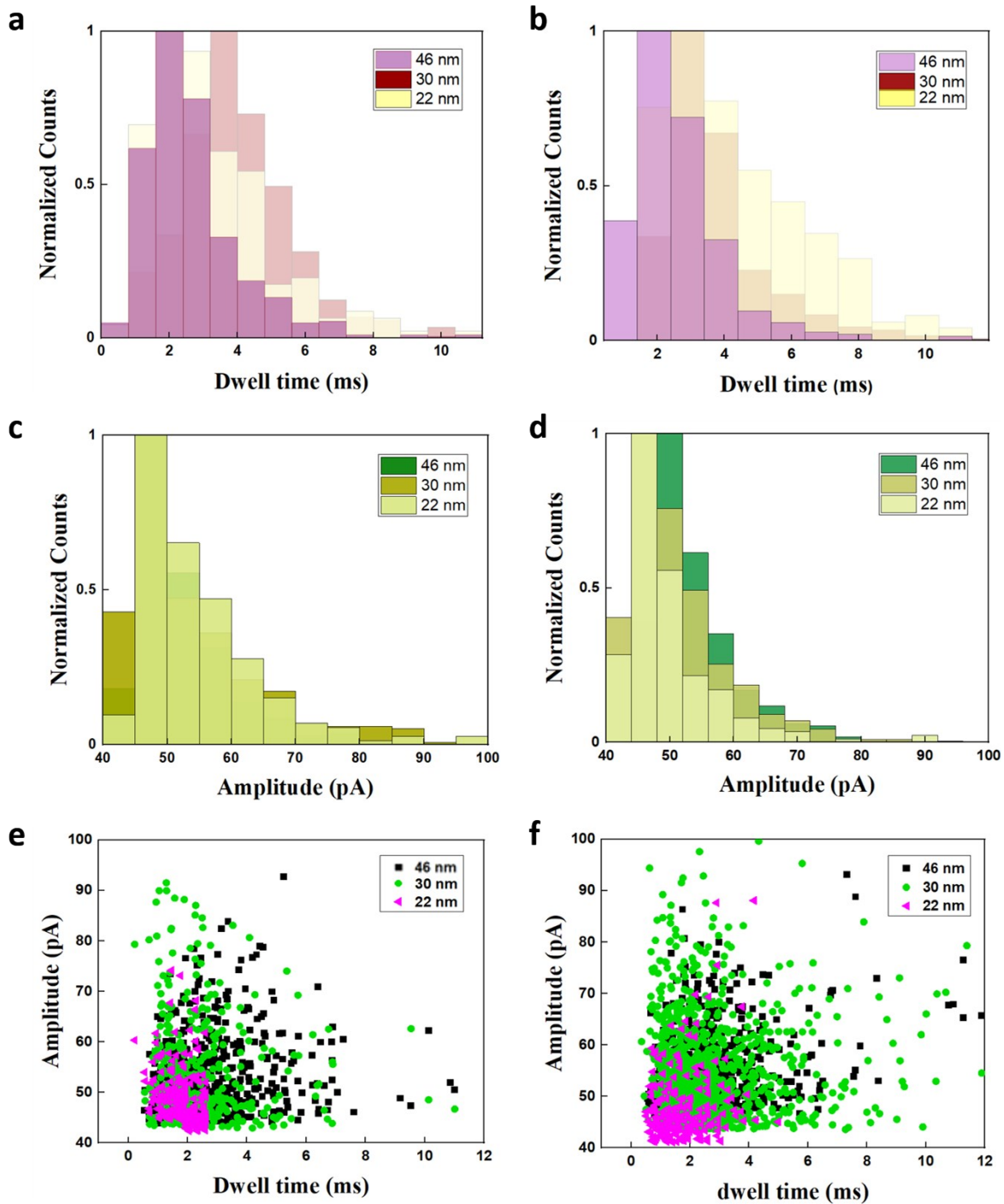


Figure S2. Dwell time and amplitude comparison between three pore sizes for two distinct depths at 500 mV applied voltage. (a and b) Dwell time distributions at 0.5 and 5 mm submersion depths, respectively. (c and d) Amplitude distributions at 0.5 and 5 mm submersion depths, respectively. (e and f) Comparison of dwell time and amplitude distributions between 0.5 and 5 mm submersion depths, respectively.

## References

1. Jing, D. & Bhushan, B. Quantification of surface charge density and its effect on boundary slip. *Langmuir* **29**, 6953–6963 (2013).